Calorimetric heats for CO and oxygen adsorption and for the catalytic CO oxidation reaction on Pt{111}

Y. Y. Yeo, L. Vattuone,[a] and D. A. King
Department of Chemistry, University of Cambridge, Lensfield Road, Cambridge CB2 1EW, United Kingdom

(Received 20 August 1996; accepted 26 September 1996)

Single crystal adsorption calorimetry was applied to investigate the heats of adsorption of CO and oxygen and the reaction heats for the CO oxidation process on Pt{111} at room temperature. Both sticking probabilities and heats of adsorption for CO and oxygen are presented as a function of coverage. These results are used to interpret the subsequent measurements taken for the CO oxidation process on the same surface. The initial heats of adsorption of CO and oxygen on Pt{111} are 180 ± 8 and 339 ± 32 kJ/mol, respectively. In addition the pairwise lateral repulsive interaction between CO molecules in a $(\sqrt{3}\times\sqrt{3})R30°$ ordered layer at $\theta=1/3$ is found to be 4 kJ/mol. A detailed Monte Carlo modeling of the dissociative adsorption and sticking probability of oxygen on Pt{111} is performed. The initial rapid fall in heat is attributed to adsorption on defect sites, and subsequent adsorption on the planar {111} surface proceeds with a third neighbor interaction energy between the oxygen adatoms $\omega_3\sim22$ kJ/mol. When gaseous CO reacts with preadsorbed oxygen adatoms, the CO_2 produced has an excess energy of 16 ± 8 kJ/mol. © *1997 American Institute of Physics.* [S0021-9606(97)02601-9]

I. INTRODUCTION

The adsorption of CO on platinum surfaces has been extensively studied due to its industrial importance in various catalytic processes, such as Fischer–Tropsch synthesis[1] and CO oxidation in car exhaust catalytic converters.[2] Many surface science techniques have been employed to investigate and understand this chemisorption process, including low energy electron diffraction (LEED),[3] thermal desorption spectroscopy (TDS),[3,4] electron energy loss spectroscopy (EELS),[4] molecular beam scattering,[5] reflection-absorption infrared spectroscopy (RAIRS),[6] and work function measurements.[3] Isosteric heat measurements (derived from work function, TDS and LEED data) were performed by Ertl *et al.*[3] and we compare these with our present study. Comparison can also be made with the theoretical predictions of Ray and Anderson[7] based on a molecular orbital study. They reported different binding energies for the possible coordination sites of CO on Pt{111} ranging from 180 (one fold sites) to 112 kJ/mol (high-coordinate sites). The calorimetric technique was applied to CO on Pt{110} by Wartnaby and co-workers,[8] who found an initial heat of adsorption of 183 ± 7 kJ/mol.

The adsorption of oxygen on Pt surfaces is central to understanding catalytic oxidation processes taking place on transition metal surfaces. However, no consensus has been reached on the magnitude of the adsorption energy, and some debate has been raised as to whether the saturation coverage of oxygen on Pt{111} is 0.25 or 0.50 ML. Many techniques have been employed, including LEED,[9,10] molecular beam scattering,[11] thermal desorption,[12] high resolution EELS,[13] and Auger electron spectroscopy (AES).[10,12] Gland *et al.*[12] investigated the O/Pt{111} system using thermal desorption, energy electron loss spectroscopy, and ultraviolet photoemission, and associated the desorption for atomic oxygen at 700 K with an initial desorption energy of about 460 kJ/mol. Ray and Anderson[14] performed molecular orbital calculations giving binding energies for oxygen on Pt{111} of 4.15 eV (400 kJ/mol), 3.08 and 3.01 eV (290 kJ/mol) for the atop, bridge, and threefold sites, respectively. The higher stability for the atop site is surprising. Materer *et al.* performed a detailed LEED structural analysis for the Pt{111}-$p(2\times2)$-O system and found that the most favorable adsorption sites for the O adatoms are the face-centered-cubic (fcc) hollow sites, with some buckling induced in both the top and second layer metal atoms.[9] A recent *ab initio* DFT-GGA calculation by Ge *et al.*[15] revealed that on Pt{100} the bridge site is most stable at a coverage of 0.5 ML, followed by the fourfold hollow site, and that the atop site is the least stable. The energies are calculated by the GGA method to be 3.8, 3.1, and 2.8 eV, respectively.[15] Wartnaby *et al.*[8] previously determined calorimetric heats for oxygen on Pt{110}, and reported an initial heat of 335 kJ/mol.

Campbell *et al.*[10] found that dissociative oxygen adsorption occurs with an initial sticking probability that decreases from 0.06 at 300 K to 0.025 at 600 K. Regarding the saturation coverage of oxygen adsorption on Pt{111}, most authors agree on a value of 0.25 ML,[10–12] while others report a value of 0.5 ML.[16] This discrepancy may be accounted for by several complicating factors: the low initial sticking probability and its rapid decrease with coverage; the marked effect of surface topology on adsorption kinetics; and the high reaction probability of background gases (CO and H_2) with the adsorbed oxygen atoms.

The oxidation of CO on transition metals has received considerable attention over the past few decades. In Sec. III C of this article, we present results for the simultaneous determination of the coverage-dependent sticking probability

[a]Present address: Dipartimento di Fisica, Università di Genova, Via Dodecaneso 33, Genova, Italy.

 0021-9606/97/106(1)/392/10/$10.00

and surface reaction heat for gaseous CO interacting with preadsorbed O adatoms. By extracting the appropriate energetic data from both of the above studies, the excess excitation energy of gaseous CO_2 formed from the surface reaction is deduced. Detailed studies of the reaction scheme,[16] the dynamics,[17–19] and the energy of the departing CO_2 (Ref. 20) have previously been performed to understand the process. CO_2 molecules produced on Pt{111} can be liberated into the gas phase with translational, vibrational, and rotational energies in excess of that expected from the substrate temperature. The excess translational energy alone can be as high as 56 kJ/mol in the reaction of atomic oxygen with CO on Pt{111},[21] although time of flight results suggest that certain conditions may give rise to highly excited products accompanied by thermally accommodated molecules.[22] The characteristic vibrational temperature of CO_2 produced on polycrystalline foils is also reported to be higher than the substrate temperature T_s, ranging from about $T_v=1250$ K with $T_s=750$ K (Ref. 23) to 1900 K with $T_s=1000$ K,[24] and is generally found to increase with surface temperature.

The first and only direct calorimetric study of the heat of a reaction, that of CO oxidation on Pt{110}, was carried out fairly recently.[25] It revealed that, when CO is dosed onto a saturated oxygen overlayer, the product CO_2 molecules remove only 9 ± 17 kJ/mol more energy than expected for thermally accommodated molecules. However, when gaseous oxygen reacts with predosed CO, the product molecules remove as much as 52 ± 21 kJ/mol of excess energy. Due to the low initial sticking probability of oxygen on Pt{111}, it has only been possible[26] to react CO with preadsorbed oxygen in our present study on this surface.

II. EXPERIMENT

The apparatus for single crystal adsorption calorimetry (SCAC) has been described in detail elsewhere,[27] including the significant improvements made more recently.[28] Therefore, only a very concise description is given here. SCAC is a powerful new surface science tool because it may be applied to systems that adsorb reversibly or irreversibly to obtain accurate coverage-dependent adsorption and reaction energies. The ultrahigh (UHV) system is equipped with an experimental chamber, a preparation chamber, and a molecular beam source; experimental and preparation chambers have a base pressure of 8×10^{-11} mbar or better.

A major feature of the calorimeter is the nature of the single crystal sample used. It is only $\sim$2000 Å thick, and is $\sim$5 mm in diameter. This thin crystal is mounted on a Pt polycrystalline ring such that only the rims are in contact with the ring: the central 4 mm region is freely supported. Gas doses are supplied to the central $\sim$2-mm-diameter region of the crystal via a molecular beam source, pulsed at a repetition period of about 2.5 s and a pulse length of 50 ms. The heat liberated by adsorption during each pulse causes a measurable temperature rise because of the low heat capacity of the sample compared to its surface area. A thin coating of amorphous carbon is deposited on the back face of the crystal to increase its emissivity and the temperature rise of the crystal due to gas adsorption is then monitored remotely with a broadband Hg–Cd–Te detector. Calibration of these heat signals is then performed *in situ* with a laser pulse of known power that simulates the spatial and temporal profiles of the molecular beam.

Gas molecules that do not adsorb are scattered back into the gas phase, producing a partial-pressure rise in the experimental chamber. This is monitored with a mass spectrometer, and thus the relative adsorbed amount or sticking probability can be inferred. The King and Wells technique[29] is used, based on a comparison with the scattered flux from an inert (gold) surface. The beam intensity, typically of the order of $\sim10^{12}$ molecules per pulse, is calibrated absolutely with a spinning rotor gauge so that the amount adsorbed can be accurately determined at each stage and summed to give the accumulated coverage. The absolute energy is determined by laser calibration and, with the amount adsorbed, this yields an absolute molar adsorption heat for each pulse of gas. Furthermore, an absolute coverage scale is obtained against which the adsorption heat and the sticking probability can be plotted. However, when the heat of adsorption falls, desorption becomes appreciable between pulses, and finally a steady state is attained whereby the amount of gas added during each pulse is balanced exactly by the quantity of gas that desorbs between pulses. Summing the sticking contributions given by the finite sticking probability measured for each pulse thus yields an apparent coverage scale that extends indefinitely: the true coverage must reach some definite limit.

The preparation chamber is equipped with an argon ion gun, a cylindrical mirror analyzer for AES, a lamp (for heating and annealing the crystal), and LEED optics. The thin film crystal is cleaned by repeated cycles of gentle argon ion sputtering and heating to about 600 K, until no contamination (particularly carbon) can be detected by AES, and until sharp LEED spots are observed.

All results shown are the average of at least six independent experimental runs performed with 99.9995% pure oxygen and 99.97% CO (both from MG Distillers, UK) on the Pt{111} substrate held at room temperature. The error bars in the figures indicate the standard deviation between these runs, and so reflect the reproducibility of the experimental results. They do not represent the calculated absolute error; the errors for both the sticking probability and the heat of adsorption or reaction are smaller than 6%.[28]

III. RESULTS AND DISCUSSIONS

A. CO adsorption

The microcalorimetric results for CO adsorption, averaged over six experimental runs, are shown in Fig. 1. The heat of adsorption of CO at 300 K is initially 183 ± 8 kJ/mol, declining to 118 ± 19 kJ/mol at the expected saturation coverage of 0.50 ML. It is also worth noting that the gradient of the heat curve changes at about 0.36 ML coverage. This is consistent with LEED experiments[3,30] which show that room temperature adsorption yields a $(\sqrt{3}\times\sqrt{3})R30°$ ordered layer at $\theta=0.33$ ML, and a $c(4\times2)$ structure at around 0.50 ML.

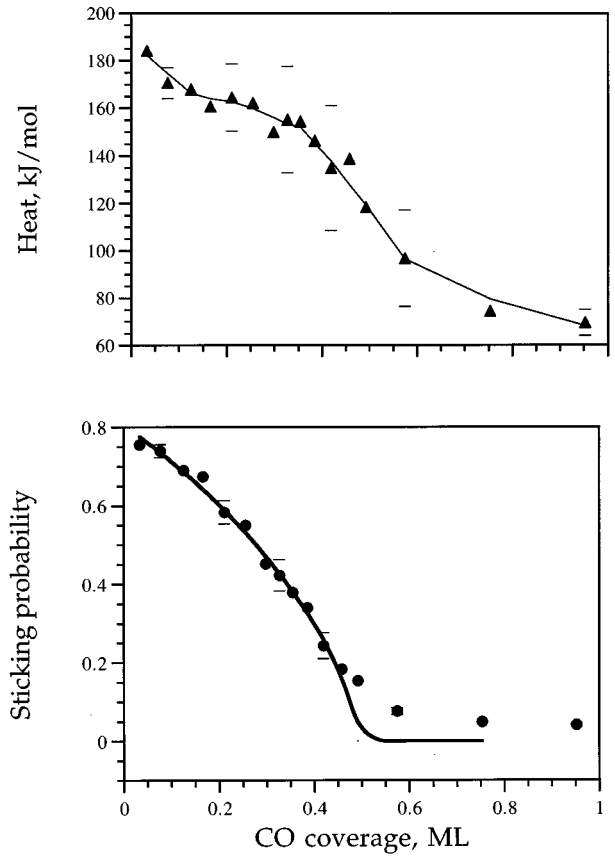

FIG. 1. Adsorption heats (▲) (above) and sticking probabilities (●) (below) for CO on the initially clean Pt{111} surface at 300 K. The bold line running through the sticking probability data shows a fit to the Kisliuk expression [Eq. (1)] indicating precursor-mediated adsorption, with $s_0=0.80$ and $K=0.55$. The coverage scale is expressed relative to a monolayer of platinum surface atoms Pt_s, equivalent to 1.5×10^{15} atoms/cm^2. The error bars given are the standard deviations between the six independent experimental runs.

The heat then falls dramatically at 0.50 ML and levels out to 65 ± 3 kJ/mol at the steady state, where desorption between pulses exactly compensates for the adsorption during the 50 ms pulses, for which we accurately measure a finite sticking probability and heat as explained above.

From the coverage-dependent heats of adsorption, a simple analysis to extract the adsorbate interaction is possible. At $\theta=0.33$ ML a $(\sqrt{3}\times\sqrt{3})R30°$ ordered layer forms as shown in Fig. 2. This corresponds to a heat of 160 kJ/mol where the heat curve flattens into a plateau in the region of 0.17–0.33 ML. At this coverage, each CO adsorbate will be surrounded by six next nearest neighbors (nnn), so the nnn interactions ω_2 can be estimated as

$$\omega_2=(q_0-q_{0.33})/6=(183-160)/6=3.8 \quad \text{(kJ/mol)},$$

where q_0 is the initial differential heat of adsorption and $q_{0.33}$ is the heat of adsorption at 0.33 ML coverage. We emphasize that the above procedure is only an approximation since the EELS and LEED results of Steininger *et al.*[4] demonstrate that a small fraction of the bridge sites is filled as the coverage increases above 0.17 ML.

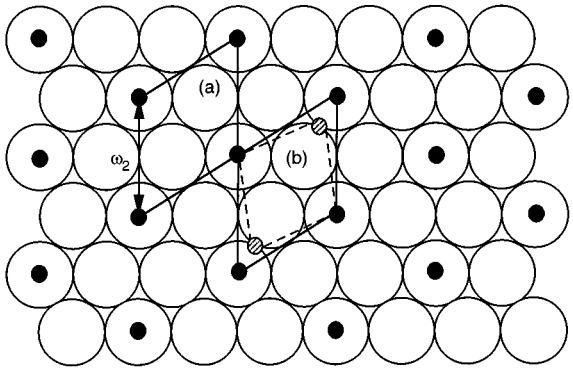

FIG. 2. (a) Plan view of the $(\sqrt{3}\times\sqrt{3})R30°$ ordered structure at $\theta=0.33$ ML. At this coverage, each CO adsorbate is surrounded by six next nearest neighbors (nnn), and the second nearest interaction is represented by ω_2 as indicated in the diagram. (b) The $(\sqrt{3}\times\sqrt{3})R30°$ ordered structure shown uniaxially compressed to give the $c(2\times4)$ structure on increasing the coverage of the CO adsorbate. The CO molecules will move away from on-top sites (filled circles) to occupy the bridge sites (shaded circles).

Similarly at $\theta=0.5$ ML, the heat of adsorption $q_{0.5}$ has fallen sharply to 118 kJ/mol corresponding to the $c(4\times2)$ structure shown in Fig. 3. Each adsorbate is now surrounded by four CO molecules on bridge sites and four CO on atop sites. The differential heat at this coverage can be written as

$$q_{0.5}=0.5q_0\ \text{(atop)}-2\omega_2-2\omega_b+0.5q_0\ \text{(bridge)}-2\omega_2-2\omega_b,$$

where $0.5\ q_0$ (atop) is the heat of adsorption on the atop sites (equivalent to the initial heat of adsorption q_0), $0.5\ q_0$ (bridge) is the heat of adsorption on the bridge sites, and ω_b is the interaction energy between an adsorbate on an atop site and one on a bridge site. We then have the expression:

$$q_0\ \text{(bridge)}-8\omega_b=83.4\ \text{kJ/mol}.$$

The sticking probability curve exhibits precursor-mediated behavior that is well fitted up to 0.5 ML by the Kisliuk expression:[31]

$$\frac{s}{s_0}=\left(1+\frac{\theta/\theta_s}{1-\theta/\theta_s}K\right)^{-1}. \tag{1}$$

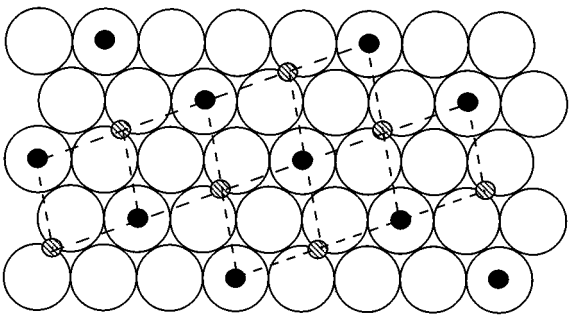

FIG. 3. Plan view of the $c(2\times4)$ ordered structure at $\theta=0.50$ ML. Each adsorbate is now surrounded by four CO molecules adsorbed on bridge sites and four CO on atop sites. The interaction energy between the CO on the on-top site and a CO on a bridge site is represented by ω_b.

Here s is the sticking probability at the instantaneous coverage θ, θ_s is the saturation coverage, s_0 is the initial sticking probability, and the parameter K describes the degree of mobility of the precursor: small positive values correspond to a highly mobile precursor while $K=1$ corresponds to an immobile precursor and hence simple Langmuir kinetics. The least-squares fit to these data gives $K=0.55$ and $s_0=0.80$. In this form, the model neglects adsorbate interactions (other than site blocking) and adlayer ordering.

The saturation coverage obtained by extrapolating the Kisliuk curve to $s=0$ is 0.53 ML, in good agreement with previous results that indicate a saturation coverage in the region of 0.50 ML.[3,5]

Above $\theta=0.50$ ML the sticking probability falls to the steady-state value, whereas the heat of adsorption remains relatively high compared to the steady-state value until a coverage of about 0.75 ML is reached. Persson *et al.*[6] performed Monte Carlo simulations on this adsorption system at high CO coverage to simulate their LEED and RAIRS data. Their LEED data showed ordered structures at $\theta=0.50$, 0.60, and 0.71 ML, but in contrast to their Monte Carlo simulation and previous results, no ordered structure was observed at $\theta=0.67$ ML. Their RAIR spectra revealed at $\theta=0.5$ ML a single sharp and intense band at 2104 cm^{-1} attributed to linearly bonded CO, and another band at 1854 cm^{-1} attributed to the bridging sites. On increasing the adsorbate coverage to $\theta=0.71$ ML, this linear band was reported to shift by only 2 cm^{-1} while considerable structure and broadening was observed in the bridge band as it gradually shifts to 1887 cm^{-1} at saturation coverage. The bridge band/atop band intensity ratio also decreases by a factor of 1.7 on going from $\theta=0.50$ to $\theta=0.71$. Persson *et al.* suggest that the compression structures formed at coverages exceeding half a monolayer of CO are formed when CO molecules at high density domain walls are shifted off atop sites (due to unbalanced repulsive CO–CO interactions) towards the bridge sites.[6] The increased local coverage of the on-top (or off-on-top) species increases the extent of dipole coupling, which tends to raise the frequency of this bridge band. Although the adsorption heats on these sites, formed from the squeezing of the $(\sqrt{3}\times\sqrt{3})R30°$ unit cell, remain relatively high, the probability of the precursor finding such a site is very low. Therefore, the sticking probability falls to almost the steady-state value at $\theta=0.50$ ML.

For the adsorption of CO on Pt{111}, isosteric heats as a function of coverage are available from a previous study by Ertl *et al.*[3] These are derived using three different techniques to specify constant coverage: the work function ($\Delta\phi$) for θ in the range of 0–0.5 ML, thermal desorption spectra (0–0.5 ML), and LEED patterns ($\theta>0.5$ ML). These data points are plotted together with the results of the present study in Fig. 4 for comparison. Their values from thermal desorption spectra are not included in Fig. 4 because the pre-exponential ν was assumed to be 10^{15} s^{-1} in order to achieve good agreement with values they obtained from the $\Delta\phi$ data. Although there is remarkably good agreement between the LEED data and the calorimetric measurements, the low coverage calorimetric data (0–0.50 ML) give heats consistently higher than the values obtained by Ertl and co-workers. This could perhaps be explained by a breakdown in the assumption[3] of a temperature invariance in the work function at fixed coverage. The LEED patterns depend uniquely on the coverage above $\theta=0.5$ ML, and could therefore be used to determine the equilibrium coverage as a function of temperature at fixed pressures. The accuracy claimed for the LEED-based heats is ±1 kcal/mol (±4.2 kJ/mol), but becomes worse near saturation.

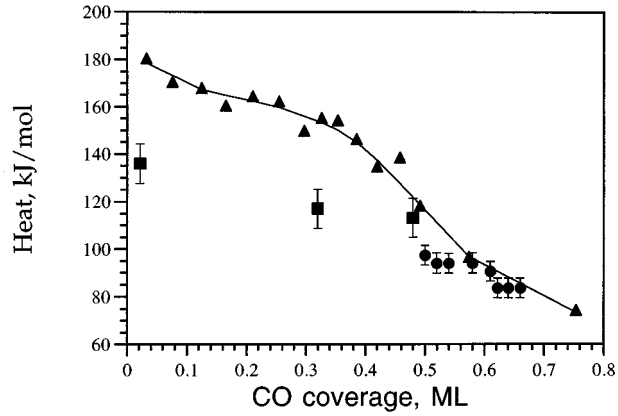

FIG. 4. The heat of adsorption of CO on Pt{111} as measured in the present study (▲) plotted together with the isosteric heats of adsorption obtained in Ref. 4. Error bars from the latter are included to give an indication of the quality of agreement between the results. The data points (■) are derived from work function measurements (for $\theta\leqslant0.5$), while the data points (●) are derived from the LEED analysis (for $\theta>0.5$). The error bars for the former are reported as ±1 kcal/mol (4.2 kJ/mol) and the latter as ±2 kcal/mol (8.4 kJ/mol).

B. Oxygen adsorption

1. Experimental results

The averaged results of seven experimental runs are shown in Fig. 5, where again the error bars indicate the standard deviation between the independent runs. The initial adsorption heat is 339 ± 32 kJ/mol, declining rapidly with coverage to only 211 kJ/mol at 0.10 ML, and flattening out to approximately 125 ± 8 kJ/mol at the steady state. Large error bars are due to a generally small sticking probability that ranges from 0.064 at zero coverage to only 0.02 in the steady-state regime.

From the initial heat of adsorption q_{O_2}, and the dissociation energy (494 kJ/mol) of oxygen in the gas phase, it is possible to extract the Pt–O bond strength at the zero coverage limit. By considering the initial heat of adsorption,

$$O_2+2\ Pt\rightarrow 2\ Pt\text{–}O,\quad q_{O_2}=339\ \text{kJ/mol},$$

we find the Pt–O bond energy to be 417 kJ/mol on clean Pt{111}. However, if, as discussed below, an initial value of about 305 kJ/mol is appropriate for the initial heat, on the planar Pt{111} surface, the Pt–O bond energy is evaluated as 400 kJ/mol. This value is comparable with a surface Ni–O bond energy of 512 kJ/mol,[32] and supports the trend that Ni surfaces have stronger adatom–metal bond energies than Pt.

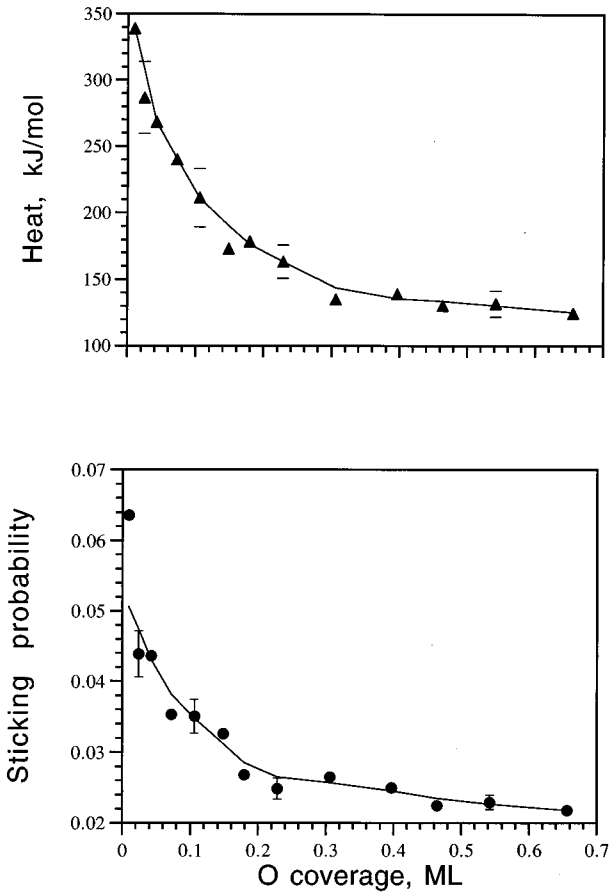

FIG. 5. Adsorption heats (▲) (above) and sticking probabilities (●) (below) for oxygen on the initially clean Pt{111} surface at 300 K. The coverage scale is expressed in monolayers of O adatoms relative to the number of Pt surface atoms.

The initial adsorption heat is considerably larger than estimates from TDS.[10] Campbell *et al.*[10] fitted their thermal desorption data with a rate constant of $\nu_d = 2.4\times10^{-2}$ $cm^2\ s^{-1}$ and an activation energy decreasing from 213 to 176 kJ/mol. There is good agreement with the adsorption energy calculated by Ray and Anderson,[14] but for the (unlikely) atop site, of about 400 kJ/mol. The present value is remarkably similar to the measurements made by Wartnaby *et al.*[8] for Pt{110} using single crystal calorimetry. The latter authors reported the initial heat for O_2 to be 332 ± 10 kJ/mol, and found that the heat declined rapidly with coverage to only 215 kJ/mol at 0.35 ML of O adatoms. In the present study, the heat drops even more rapidly: at 0.30 ML it has fallen to 135 kJ/mol.

The initial sticking probability is 0.064, in excellent agreement with the room temperature molecular beam measurement of 0.06 by Campbell *et al.*[10] At 0.25 ML coverage (Fig. 5), the sticking probability has decreased to about 0.025 and a steady-state value of below 0.02 is attained at apparent coverages exceeding 0.6 ML. From the data the true saturation coverage of this system is in the region of 0.25–0.30 ML, as expected for a single (2×2) overlayer phase as indicated by LEED structural analyses.[9] The formation of this structure is further supported by the results from our Monte Carlo simulation.

2. Monte Carlo simulation

The coverage dependence of both the sticking probability and the heat of adsorption at room temperature can be accounted for using a simple model including lateral interaction between adatoms and a precursor state for dissociative adsorption. First, however, we note that both the sticking probability and the heat of adsorption curves (Fig. 5) show abrupt drops between 0 and ~0.02 ML. This is strongly suggestive of the occupation and saturation of defect sites, such as steps. No other explanation can be offered for such a sharp fall in the sticking probability over this range. We therefore conclude that the true initial sticking probability characteristic of the planar {111} surface is 0.05, and the initial adsorption heat is 305 kJ/mol. In the Monte Carlo fitting we discount the initial 0.02 ML.

Over the coverage range 0.02–0.2 ML the differential heat of adsorption decreases continuously with increasing coverage, suggesting that the adsorbate is immobile at this temperature. If, for instance, a (3×3) overlayer could form at low coverage due to repulsive interactions at smaller interatomic spacings, a constant heat of adsorption would be observed up to a coverage of about 1/9 ML, followed by an abrupt decrease. The saturation coverage appears to be below 0.25 ML, indicating that the occupation of both the nearest neighbors and next nearest neighbors is forbidden. The main contribution to the decreasing adsorption heat therefore arises from adatoms adsorbed in third neighbor positions. When the coverage is sufficiently high a (2×2) overlayer is observed;[9] each adatom then has six adatoms in the third neighbor positions, so that the adatom–adatom interaction at that distance can be estimated to be $\sim(q_0 - q_{0.25})/6$. The magnitude of the pairwise lateral interaction energy can therefore be estimated as ~27 kJ/mol. A full Monte Carlo simulation of the coverage-dependent sticking probability and differential heat is, however, necessary to give a better estimate of the lateral interactions.

In this simulation, a 40×40 grid of {111} sites is considered. The procedure can be summarized as follows. A molecule attempts to dissociate at a random site by leaving the adatoms at the lowest possible separation, in third neighbor positions. Nearer positions are forbidden. If the random site found is already filled or if all the six third neighbor sites are occupied, the molecule will either desorb with probability $p_{\rm des}$ or seek another site with probability $(1-p_{\rm des})$; when a new site is found, the procedure is repeated. When the molecule finds the sites for dissociation, the corresponding energy is calculated. If the energy is lowered by adsorption, the molecule remains on the same site, otherwise the molecule can desorb with the probability $p_{\rm des}$ or seek another adsorption site.

The energy is calculated as follows. Each adsorbed molecule is assigned an adsorption energy (q_0) equal to the low coverage limit of $q_{\rm diff}$. For each first or second neighbor a very high repulsive contribution ($\omega_1 = \omega_2$ much greater than

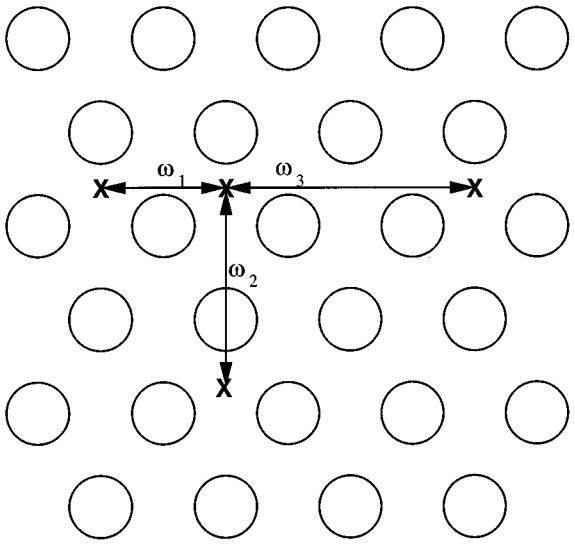

FIG. 6. Schematic diagram of the empty site array required for dissociative O_2 adsorption to occur. The platinum surface atoms on the {111} surface are represented by open circles. The crosses illustrate the three possible (atop) adsorption sites for the oxygen to fill after dissociation. ω_1, ω_2, and ω_3 label the next, second, and third nearest neighbor positions, respectively.

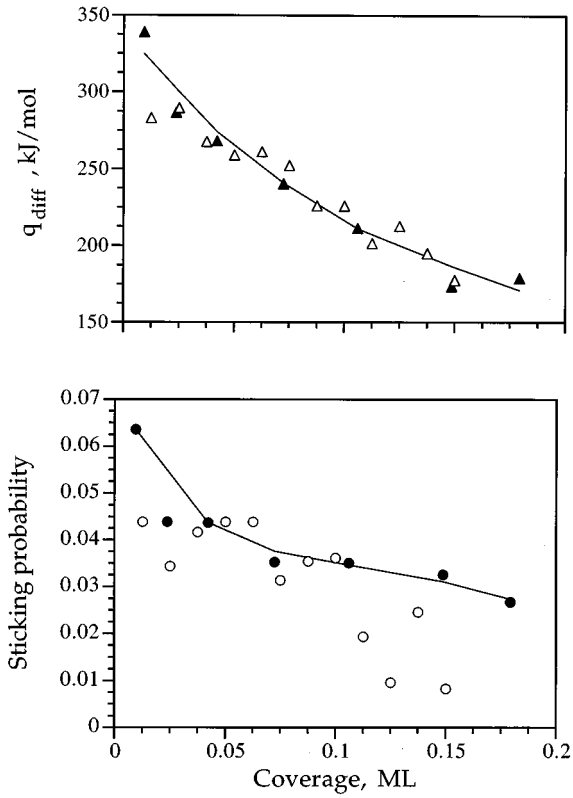

FIG. 7. The experimental differential heat q_{diff} (▲) (above) and sticking probability (●) (below) are plotted together with the results from a Monte Carlo simulation (△ and ○) with $\omega_3 \sim 22$ kJ/mol and $\omega_0 = -305$ kJ/mol. Only one equilibration step is allowed after dissociation, which is close to the immobile limit since each adatom has a hopping probability of $<10^{-2}$ in each equilibration step.

q_0) to the total energy is computed in order to prevent adsorption on these sites. Finally, the number of third neighbor adatoms is evaluated and a repulsive contribution ω_3 (see Fig. 6) is considered for each couple of adatoms. After each adsorption event, some equilibration of the lattice, giving an eventual decrease in the energy, is allowed. Since adsorption approaches the ''immobile adsorbate'' limit, the number of adatom hops allowed is small (1–10). A very high number of hops (~1000) would give an initially constant heat of adsorption and some low coverage ordered structures because each atom will look for a site where no third neighbor sites are occupied. If the number of possible hops is limited, occupation of third neighbor sites starts at a much lower coverage, thus giving a decreasing heat of adsorption.

These simulations allow for a simultaneous determination of the change in the differential heat and in the relative sticking probability as a function of coverage. In the limit of an immobile adsorbate the saturation coverage is lower than the ideal one for a (2×2) overlayer since some adatoms are already adsorbed at third neighbor sites at low coverage, thus blocking a higher number of first and second neighbor sites than in a more ordered structure. A similar situation was predicted by Roberts[33] for a {100} lattice where molecules dissociate at first nearest neighbor sites without further movement: when the coverage is sufficiently high, the approaching molecule cannot find two close vacant sites for dissociation to occur so the resulting saturation coverage is lower than 1 ML, even without repulsive interactions. In the simulations the coverage does not exceed ~0.16 ML. The maximum coverage attained is of course dependent on the number of possible adatom hops allowed after dissociation. If a large number of hops is allowed, a perfect (2×2) overlayer would be formed. However, such a calculation would be extremely time consuming, and is not, in any case, indicated by the data, since at room temperature, equilibration leads to an imperfect (2×2) structure. It is implicitly assumed that only one kind of adsorption sites exists, in agreement with LEED results,[9] and multiple occupation is forbidden.

The differential heat q_{diff} and sticking probability s are determined by performing the simulations as explained above. In all cases adsorption below 0.02 ML is attributed to defect sites, and is discounted. In the first case, the limit of an immobile adsorbate is considered. We obtain a best fit to the data with the values of $q_0 = -305$ kJ/mol and $\omega_3 \sim 22$ kJ/mol, and $s_0 = 0.05$. The experimentally observed behavior of both s and q_{diff} is very well reproduced, as shown in Fig. 7. The value of ω_3 is close to that obtained from the simple expression $(q_0 - q_{0.25})/6$, i.e., 27 kJ/mol. For comparison with the present work, the initial sticking probabilities, heats of adsorption, and pairwise lateral interaction energies for NO, CO, and O_2 adsorption on the low index planes of Pt are shown in Table I.

In the second simulation, the lattice is allowed to equilibrate for a longer time after each event. The result of this simulation is shown in Fig. 8. The heat is constant up to a coverage of ~0.10 ML. It is clear that this case approaches the limit of a ''mobile adsorbate'' corresponding to a system with a much higher mobility than the present experiment at

TABLE I. Initial adsorption heats q_0, sticking probabilities s_0, and pairwise lateral repulsion energies ω_n for the different systems (where n gives an indication of the distance of the neighboring pairs, i.e., 2: second nearest, 3: third nearest) obtained from experimental data obtained using the SCAC. In the case of NO on Pt{100}-(1×1), NO triplet formation (Ref. 36) is suggested with significant repulsion between the molecules in the same triplet (ω_t) and an even stronger repulsion between the triplet pairs (ω_{tt}).

System	s_0	q_0 (kJ/mol)	Lateral interactions ω_n (kJ/mol)
CO/Pt{100}-(1×1)[a]	0.61	225	ω_2=5
NO/Pt{100}-(1×1)[a]	0.68	225	ω_t=20 ω_{tt}=80
CO/Pt{111}[b]	0.80	180	ω_2~4
O_2/Pt{111}[b]	~0.05	~305 (planar {111} surface)	ω_3=22
CO/Pt{110}-(1×2)[c]	0.83	183	···
NO/Pt{110}-(1×2)[c]	0.87	160	···
O_2/Pt{110}-(1×2)[c]	0.34	335	···

[a]Reference 36.
[b]This work.
[c]Reference 8.

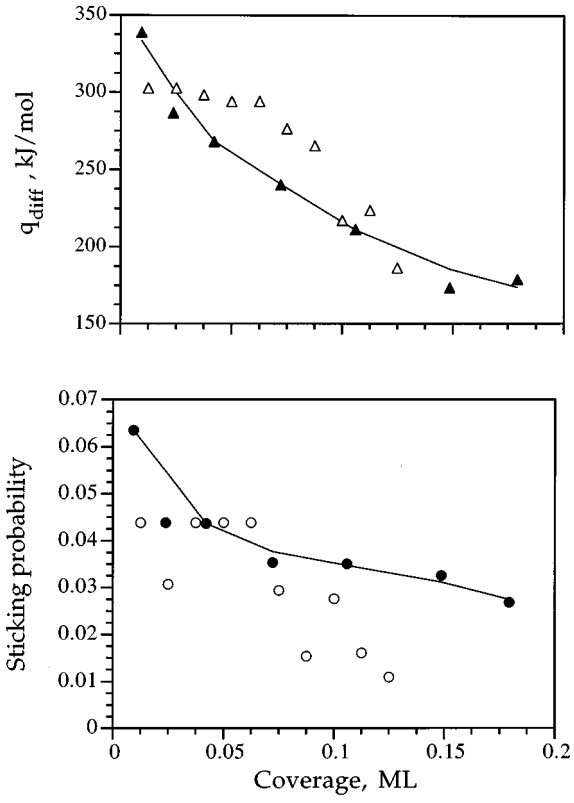

FIG. 8. Results from a Monte Carlo simulation (open triangles and circles) with ω_3~22 kJ/mol and ω_0=−305 kJ/mol are compared with the experimental (filled triangles and circles) differential heat q_{diff} (above) and sticking probability (below). One thousand equilibration steps were allowed after dissociation. These simulated results clearly correspond to a system with a much higher mobility than the experimental case.

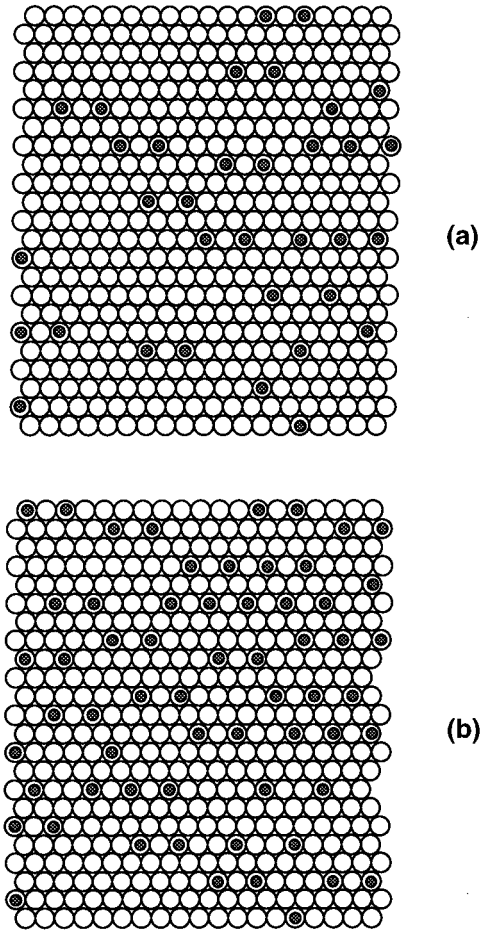

FIG. 9. (a) Snapshot of the adatom positions given by the Monte Carlo simulations in Fig. 7 at 0.08 ML coverage. The platinum surface atoms are represented by open circles and the O adatoms are represented by filled circles. (b) Snapshot of the adatom positions given by the Monte Carlo simulations in Fig. 8 at 0.15 ML coverage. The atoms are locally ordered in a (2×2) overlayer, but some of them occupy out-of-phase sites, thus preventing the complete formation of an ordered overlayer.

room temperature. It is not a good description of the 300 K SCAC data. Similar findings were reported in investigations of NO and oxygen dissociative adsorption on Ni{100}.[32] Wartnaby[34] found that a plateau in the coverage-dependent heat of adsorption for oxygen adsorption on Ni{100} is extended to higher coverages when the temperature is increased, thus allowing for a better equilibration of the adlayer. For the same reason, structures exhibiting long range order require high temperature to be equilibrated.

The first simulation is consistent with the appearance of a (2×2) overlayer at high coverage and disorder at low coverage. Figure 9 shows snapshots of adatom positions at two different coverages: 0.08 and 0.15 ML. At low coverage adatoms are adsorbed randomly but some of them have two or three adatoms in third neighbor positions, therefore yielding an average heat lower than expected for a fully equilibrated surface. At 0.15 ML adatoms are locally ordered into (2×2) structures but some of them occupy out of phase sites, thus preventing the formation of a completely ordered overlayer.

A final comment concerning the role of the precursor in

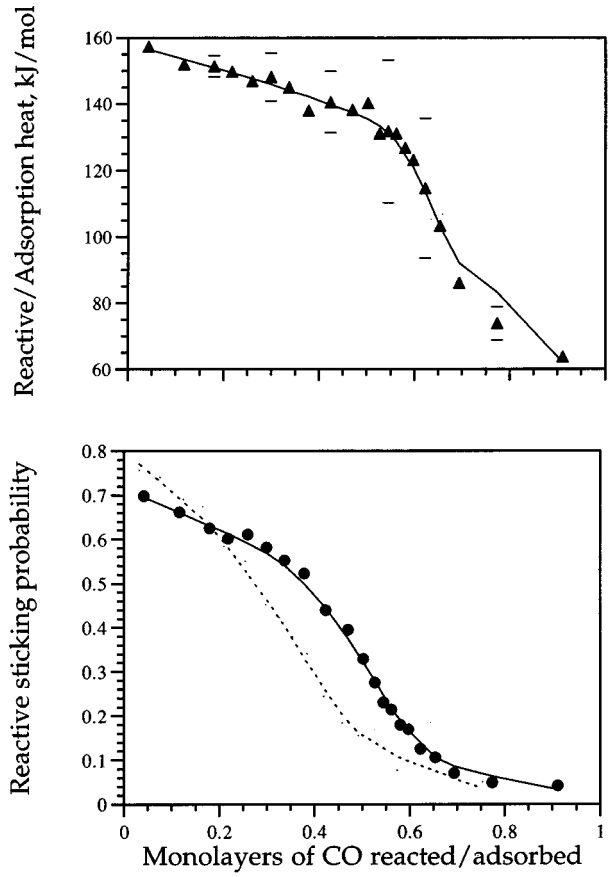

FIG. 10. Heat of reactive adsorption (▲) (above) and sticking probability (●) (below) for CO and a Pt{111} surface previously saturated with oxygen atoms. The coverage scale is expressed in terms of the amount of CO adsorbed and reacted.

dissociative adsorption is appropriate. The value of s changes by only 25% in the range of coverage 0.02–0.15 ML. Such a moderate decrease requires the precursor state to play some role in the adsorption process. The value of $p_{\mathrm{des}} \sim 0.25$ required to produce a good fit for the coverage-dependent sticking probability supports this conclusion. A similar but not negligible role for the precursor was found for oxygen dissociation on Ni{100}.[32]

C. CO oxidation

The reaction between CO and oxygen was investigated by the addition of CO to the Pt{111} surface previously saturated with a molecular beam dose of oxygen molecules equivalent to an ambient exposure of 28 L. Seven independent experimental runs were averaged to give the results shown in Fig. 10. The calorimetric results for the addition of CO are presented as a function of CO adsorbed and reacted. The initial heat of reaction is directly measured to be 157 ± 2 kJ/mol, falling gradually to 123 ± 21 kJ/mol at ~ 0.6 ML. A sharp decrease then takes place between ~ 0.60 and 0.70 ML, and when 1.0 ML CO is reached, the heat levels out to a steady-state value of about 55 kJ/mol. As the CO saturation coverage on the clean surface is only 0.5 ML, it is evident that about half of the CO adsorbed must have reacted with oxygen adatoms. Even if all CO adsorbed in a pulse were to react, it is possible that the heat measured during the molecular beam pulse corresponds simply to CO adsorption if the reaction occurs on a timescale longer than that of the measurement. Any estimate of the excess energy of the departing CO_2 product will therefore yield a lower limit to the true value.

The initial reactive sticking probability for CO is surprisingly high ($s_0 = 0.70$) and remains consistently higher than that for the clean surface (Fig. 1) even though the surface has been presaturated with oxygen adatoms. If all the preadsorbed O reacts to form CO_2, we would expect 0.25 to 0.30 ML of CO to react and a further 0.5 ML to adsorb, giving a total of 0.75–0.8 ML, as shown by the sticking probability curve in Fig. 10. The steady-state sticking probability for CO on the O-precovered surface is only 0.04, and is reached at a coverage of 0.77 ML. This steady-state value is indistinguishable from the adsorption of CO on the clean Pt{111} surface. This is an indication that the O adlayer was completely removed in the reaction. Due to the small sticking probability for oxygen on a CO-predosed Pt{111} surface, the only coadsorption study that could be performed with the SCAC was to first predose oxygen onto a clean Pt{111}.

The reaction that needs to be considered is

$$\mathrm{CO_{(g)} + O_{(ad)} \rightarrow CO_{2(g)}}.$$

The heat of reaction $\Delta_r H$ is thus

$$\Delta_r H = \Delta_f H\{\mathrm{CO_{2(g)}}\} - \Delta_f H\{\mathrm{CO_{(g)}}\} - \Delta H\{\mathrm{O_{(Pt)}}\},$$

which can be evaluated from the heats of formation $\Delta_f H$ of gaseous CO_2 and CO at 298 K and 1 atm pressure, i.e., -393.5 and -110.5 kJ/mol, respectively,[16] and the measured adsorption heat for O, $\Delta H\{\mathrm{O_{(Pt)}}\}$. The enthalpy change due to expansion to low pressure, which is zero for an ideal gas, is ignored. Since the clean Pt{111} is presaturated with oxygen, the $\Delta H\{\mathrm{O_{(Pt)}}\}$ value is taken to be the steady-state adsorption heat of oxygen (110 ± 8 kJ/mol) on the surface as shown in Fig. 5. The magnitude of the calculated heat for the initial reaction ($-\Delta_r H$) is therefore 173 ± 8 kJ/mol, this being the quantity that would be measured calorimetrically should the CO_2 leave the surface without excess internal or translational energy.

From Fig. 10, we see the heat measured for the initial reaction of CO with the oxygen overlayer is only 157 ± 2 kJ/mol and it was extremely reproducible over seven independent experimental runs. This is lower than expected for CO_2 molecules desorbing at the same temperature as the surface, i.e., 300 K, and we conclude that CO_2 is produced in the gas phase with an average excess energy of 16 ± 8 kJ/mol. These data clearly indicate a certain degree of excitation, and are at first examination in qualitative agreement with previous work.[17,19,21,22]

It was established some years ago that the mode of reaction depends on which gas, O_2 or CO, is preadsorbed. In a RAIRS study, Shigeishi and King found that, when a surface saturated with CO at 300 K was exposed to oxygen, the CO band intensity decreases as the oxidation proceeds but with-

out a shift in frequency.[26] However, when a surface preadsorbed with oxygen at 300 K is exposed to CO, the CO band first appears at 2081 cm^{-1} and then shifts continuously to the saturation value identical to that of CO adsorption alone. In the present study, a high initial sticking probability (0.70) is measured for the adsorption of CO on an adlayer of preadsorbed oxygen atoms, while effectively no sticking is observed for oxygen on a presaturated surface of CO. When the surface is crowded by a uniform adlayer of CO, approaching oxygen molecules have a very low probability to find free sites for dissociation and hence react to form CO_2. Once O_2 *is* adsorbed, further oxygen adsorption occurs on the free sites generated by the CO oxidation, leading to the formation of islands of adsorbed oxygen, the reaction being largely restricted to the boundaries between CO and oxygen islands; the local CO coverage remains constant. However, preadsorbed O adatoms do not inhibit CO adsorption, and CO is randomly adsorbed, reacting with adjacent oxygen adatoms to produce CO_2.

Becker and co-workers[35] performed time of flight (TOF) measurements with a Pt{111} film grown epitaxially on a mica substrate. In their study, a chopped molecular beam of CO was directed at the sample held at 880 K, which was maintained in an ambient pressure of oxygen. They reported that the CO_2 collected at normal incidence and at 45° from the sample had equivalent excess translational energies of 15.0 and 3.2 kJ/mol, respectively. A more recent TOF study by Poehlmann *et al.*[22] revealed an excess kinetic energy of the desorbing CO_2 molecules of 0.4 eV (39 kJ/mol) with bimodal angular and velocity distributions. In this work the reaction was studied at steady state at 550 K, where CO and O_2 are dosed continuously onto the surface. It is not possible to compare our excess energy value with the average translational energy directly for several reasons. First, we measure the *integrated* excess energy, not that partitioned into each of these modes. Second, the technique we have adopted (whereby preadsorbed oxygen is allowed to react with CO from the molecular beam) can give rise to energetically different CO_2 products from reactions whereby CO and O_2 are simultaneously dosed. In earlier work it was shown that more highly excited CO_2 desorbed from the Pt{110} at room temperature by reacting oxygen with predosed CO than vice versa.[25] The fast component of CO_2 was attributed to hot oxygen atoms that react quickly with preadsorbed CO and the slow component to oxygen atoms that have become accommodated to the surface before reaction with diffusing CO. Finally, a major difference in substrate temperature can also explain the difference in the energy distribution of the CO_2 products.

In addition to the excess energy partitioned into the translational motion of the CO_2 molecules produced in the oxidation reaction, further excess energy can be channelled into *vibrational* and *rotational* degrees of freedom. Uetsuka *et al.*[20] detected CO_2 molecules produced by CO oxidation on Pt{111} that were vibrationally excited (especially into antisymmetric stretch modes) compared with those desorbed from a polycrystalline Pt foil by molecular beam and infrared chemiluminescence techniques. Other investigations have also been conducted to obtain information on the internal energy of the CO_2 product but these have concentrated on less well-defined surfaces, such as Pt polycrystalline foils. Brown and Bernasek[24] found vibrational temperatures of 1270–1060 K (8.8–10.6 kJ/mol), that decrease with increasing oxygen coverage, for CO_2 desorbing from a Pt foil at 800 K. Coulston and Haller[18] found a Boltzmann temperature of ~1500 K for the vibrational energy of CO_2 molecules produced on a Pt foil held at 800 K. Other work performed on Pt foils[23,24] further indicates both rotational and vibrational excitation.

IV. CONCLUSION

The initial heats of CO and oxygen on Pt{111} at 300 K are determined calorimetrically to be 180 ± 19 and 308 ± 32 kJ/mol, respectively. From the coverage-dependent heat of adsorption, the CO–CO second nearest neighbor interaction energy is also estimated. Initial O_2 adsorption at a higher heat up to 0.02 ML is attributed to surface defects.

The initial sticking probabilities of CO and oxygen on Pt{111} are 0.76 and 0.05, respectively, whereas the initial sticking probability of CO on a surface that was previously saturated with oxygen remains as high as 0.70. The curvature of the sticking probability versus coverage curve of CO on clean Pt{111} is well fitted by the Kisliuk expression, pertinent to precursor-mediated uptake kinetics. The sticking probability for oxygen declines monotonically with coverage.

The CO oxidation process was investigated by reacting CO pulses from the molecular beam source with O adatoms that preadsorbed onto the surface. By comparing the initial measured reaction heat, 157 kJ/mol, with that expected for a reaction that forms a CO_2 product with no excess energy, we find that CO_2 formed on this surface must depart the surface with a minimum average excess energy of 16 ± 8 kJ/mol. Like the reaction heat, the sticking probability for the CO oxidation process remains consistently higher than that for the CO on the clean surface.

ACKNOWLEDGMENTS

The UK EPSRC is acknowledged for an equipment grant and Trinity College, Cambridge, is acknowledged for a studentship for one of the authors (Y.Y.Y.). A second author (L.V.) acknowledges Fondazione Angelo della Riccia for a fellowship. The authors thank Jacques Chevallier from Aarhus University, Denmark, for supplying the thin film Pt{111} crystals.

[1] H. P. Bonzel and H. J. Krebs, Surf. Sci. **117**, 639 (1982).
[2] C. H. F. Peden, D. W. Goodman, D. S. Blair, P. J. Berlowitz, G. B. Fisher, and S. H. Oh, J. Phys. Chem. **92**, 1563 (1988).
[3] G. Ertl, M. Neumann, and K. M. Streit, Surf. Sci. **64**, 393 (1977).
[4] H. Steininger, S. Lehwald, and H. Ibach, Surf. Sci. **123**, 264 (1982).
[5] J. Liu, M. Xu, T. Nordmeyer, and F. Zaera, J. Phys. Chem. **99**, 6167 (1995).
[6] B. N. J. Persson, M. Tüshaus, and A. M. Bradshaw, J. Chem. Phys. **92**, 5034 (1990).
[7] N. K. Ray and A. B. Anderson, Surf. Sci. **119**, 35 (1982).
[8] C. E. Wartnaby, A. Stuck, Y. Y. Yeo, and D. A. King, J. Phys. Chem. **100**,

12483 (1996).
[9] S. Materer, U. Starke, A. Barbieri, R. Döll, K. Heinz, M. A. Van Hove, and G. A. Somorjai, Surf. Sci. **325**, 207 (1995).
[10] C. T. Campbell, G. Ertl, H. Kuipers, and J. Segner, Surf. Sci. **107**, 220 (1981).
[11] D. R. Monroe and R. P. Merrill, J. Catal. **65**, 461 (1980).
[12] J. L. Gland, B. A. Sexton, and G. B. Fisher, Surf. Sci. **95**, 587 (1980).
[13] A. Cudok, H. Froitzheim, and G. Hess, Surf. Sci. **307–309**, 761 (1994).
[14] N. K. Ray and A. B. Anderson, Surf. Sci. **119**, 35 (1982).
[15] Q.-F. Ge, P.-J. Hu, D. A. King, M.-H. Lee, J. A. White, and M. C. Payne (unpublished).
[16] K. Schwaha and E. Bechtold, Surf. Sci. **65**, 277 (1977).
[17] C. T. Campbell, G. Ertl, H. Kuipers, and J. Segner, J. Chem. Phys. **73**, 5862 (1980).
[18] G. W. Coulston and G. L. Haller, J. Chem. Phys. **95**, 6932 (1991).
[19] R. L. Palmer and J. N. Smith, Jr., J. Chem. Phys. **60**, 1453 (1974).
[20] H. Uetsuka, K. Watanabe, and K. Kunimori, Chem. Lett. **8**, 633 (1995).
[21] C. B. Mullins, C. T. Rettner, and D. J. Auerbach, J. Chem. Phys. **95**, 8649 (1991).
[22] E. Poehlmann, M. Schmitt, M. Hoinkes, and H. Wilsch, Surf. Sci. **287**, 269 (1993).
[23] D. A. Mantell, K. Kunimori, S. B. Ryali, G. L. Haller, and J. B. Fenn, Surf. Sci. **172**, 281 (1986).
[24] L. S. Brown and S. L. Bernasek, J. Chem. Phys. **82**, 2110 (1985).
[25] C. E. Wartnaby, A. Stuck, Y. Y. Yeo, and D. A. King, J. Chem. Phys. **102**, 1855 (1995).
[26] R. A. Shigeishi and D. A. King, Surf. Sci. **75**, L397 (1978).
[27] C. E. Borroni-Bird and D. A. King, Rev. Sci. Instrum. **62**, 2177 (1991).
[28] A. Stuck, C. E. Wartnaby, Y. Y. Yeo, and D. A. King, Surf. Sci. **349**, 229 (1996).
[29] D. A. King and M. G. Wells, Proc. R. Soc. Ser. A **339**, 245 (1974).
[30] Y.-T. Wong and R. Hoffmann, J. Phys. Chem. **95**, 859 (1991).
[31] P. Kisliuk, Surf. Sci. **64**, 43 (1977).
[32] L. Vattuone, Y. Y. Yeo, and D. A. King, J. Chem. Phys. **104**, 8096 (1996).
[33] J. K. Roberts, *Some Problems in Gas Adsorption* (Cambridge University Press, Cambridge, 1939).
[34] C. E. Wartnaby, Ph.D. thesis, University of Cambridge, 1995.
[35] C. A. Becker, J. P. Cowin, L. Wharton, and D. J. Auerbach, J. Chem. Phys. **67**, 3394 (1977).
[36] Y. Y. Yeo, L. Vattuone, and D. A. King, J. Chem. Phys. **104**, 3810 (1996).